

Forward heavy flavour production in pp collisions at LHC and intrinsic quark components in proton

G. I. Lykasov¹, V. A. Bednyakov¹, A. F. Pikelner¹ and N. I. Zimin^{1,2}

¹ Joint Institute for Nuclear Research - Dubna 141980, Moscow region, Russia

²CERN, 1211, Geneva 23, Switzerland

Abstract

The LHC data on the forward heavy flavour hadron production can be a new unique source for estimation of intrinsic charm and bottom contributions to the proton. For example, we analyze the forward heavy baryon production, namely Λ_b -baryon, within the soft QCD quark gluon string model and present the predictions for observables which could be measured at the LHC. We also present some predictions for the D -meson production in pp collisions made within the perturbative QCD including the intrinsic charm in the proton that can be verified at the LHC.

1. Introduction

There are successful phenomenological approaches to description of the soft hadron-nucleon, hadron-nucleus and nucleus-nucleus interactions at high energies based on the Regge theory and the $1/N$ expansion in QCD. For example, they are the quark-gluon string model (QGSM) [1] and the dual parton model (DPM) [2]. The main components of these models are the parton distributions in hadrons (PDF) and the fragmentation functions (FF), which describe fragmentation of quarks to hadrons. The PDF and FF are expressed in terms of intercepts of the Regge trajectories $\alpha_R(0)$.

In these models the largest uncertainty in the calculations of the yields of heavy flavours is due to the absence of any reliable information on the transfer momentum t dependence of the Regge trajectories of heavy quarkonia ($Q\bar{Q}$). If the $Q\bar{Q}$ trajectories as assumed to be linear, the intercepts turn out to be low, for example, $\alpha_\psi(0)$ is around -2 and $\alpha_{\Upsilon}(0)$ is around -8. As a result, the yield is very uncertain and decreases very rapidly with increasing quark mass. Furthermore, any knowledge of the t -dependence for $\alpha_{(Q\bar{Q})}(t)$ in the region $0 \leq t \leq M_{(Q\bar{Q})}^2$ and estimations of their intercepts become especially important for quantitative predictions.

On the other side, to reduce the above-mentioned uncertainties, fix the Regge trajectories of the bottom $b\bar{b}$ -mesons and get information about quark and diquark fragmentation functions into heavy baryons one should compare relevant QGSM predictions with the LHC experimental data. Therefore the first goal of this paper is to present and discuss some predictions, for example, for the production of the

beauty Λ_b -baryon and charmed D -meson in pp collisions. The second goal of this paper is to discuss the possibility of observing the so-called *intrinsic* quark components in pp collisions at the LHC energies [3]-[9]. The idea of the intrinsic charm existence in the proton was first put forward thirty years ago by S.Brodsky with coauthors [10, 11]. They assumed the 5-quark state $uudcc\bar{c}$ in the proton (Fig. 1).

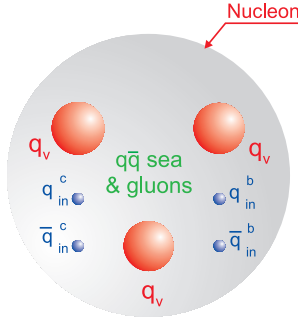


Figure 1: Schematic presentation of a nucleon consisting of three valence quarks q_v , quark-antiquark $q\bar{q}$ and gluon sea, and pairs of the intrinsic charm ($q_{in}^c\bar{q}_{in}^c$) and intrinsic bottom quarks ($q_{in}^b\bar{q}_{in}^b$).

Later some other models were developed. One of them assumes the quasi-two-body state $\bar{D}^0(u\bar{c})\bar{\Lambda}_c^+(udc)$ in the proton, see for example [3] and references therein. In [3]-[5] a probability to find the intrinsic charm in the proton was assumed to be from 1 to 3.5 percent. The probability of the intrinsic bottom in the proton is suppressed by a factor $m_c^2/m_b^2 \simeq 0.1$ [12], where m_c and m_b are the masses of the charmed and bottom quarks. Nevertheless, it was also shown that the intrinsic charm in the proton can result in a sizable contribution to the forward charmed meson production [13].

When the distribution of the intrinsic charm or bottom in the proton is similar to the valence quark distribution, then the production of the charmed (bottom) mesons or charmed (bottom) baryons in the fragmentation region is similar to the production of pions or nucleons.

However, the amount of this production yield depends on the probability to find the intrinsic charm or bottom in the proton, but this amount looks too small. In this paper we continue our study of the forward heavy flavour production in pp collisions at LHC energies published in [14, 15] and present some estimations for the contribution of the intrinsic charm and bottom to the inclusive spectra of charmed and beauty baryons and mesons. In the next section the general formalism based on the QGSM for the forward hadron production in pp collisions at high energies is presented briefly. In the first part of the section **Results and discussion**, we present the predictions for the Λ_c and Λ_b production in pp collisions at the LHC obtained within the QGSM without inclusion of the intrinsic charm and bottom in the proton. Then, in the second part of this section some estimations of the intrinsic charm and bottom contributions to the forward production of heavy mesons

and baryons in pp collisions are discussed. Finally, we give some recommendation for the forward LHC experiments to find the information on the quark intrinsic components in the proton.

2. General formalism of the QGSM

The general form for the invariant inclusive hadron spectrum within the QGSM [15, 2] is

$$E \frac{d\sigma}{d^3\mathbf{p}} \equiv \frac{2E^*}{\pi\sqrt{s}} \frac{d\sigma}{dxdp_t^2} = \sum_{n=1}^{\infty} \sigma_n(s) \phi_n(x, p_t), \quad (1)$$

where E, \mathbf{p} are the energy and the three-momentum of the produced hadron h in the laboratory system (l.s.); E^*, s are the energy of h and the square of the initial energy in the c.m.s. of the pp -system; x, p_t are the Feynman variable and the transverse momentum of h ; σ_n is the cross section for production of the n -Pomeron chain (or $2n$ quark-antiquark strings) decaying into hadrons, which are calculated within the quasi-“eikonal approximation” [16]; $n = 1$ corresponds to the left graph in Fig. 2, and $n > 1$ corresponds to the right graph in Fig. 2.

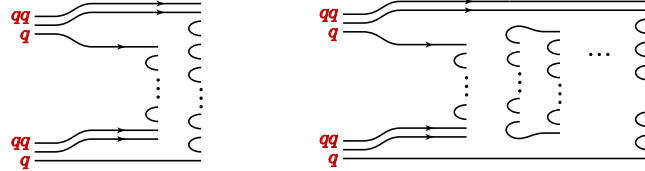


Figure 2: The one-cylinder graph (left) and the multicylinder graph (right) for the inclusive $pp \rightarrow hX$ process.

The function $\phi_n(x, p_t)$ is the convolution of the quark (diquark) distributions and the FF [15, 2, 17]:

$$\begin{aligned} \phi_n^{pp}(x) = & F_{qq}^{(n)}(x_+) F_{q_v}^{(n)}(x_-) + F_{q_v}^{(n)}(x_+) F_{qq}^{(n)}(x_-) + \\ & 2(n-1) F_{q_s}^{(n)}(x_+) F_{\bar{q}_s}^{(n)}(x_-), \end{aligned} \quad (2)$$

where $x_{\pm} = \frac{1}{2}(\sqrt{x^2 + x_t^2} \pm x)$, and

$$F_{\tau}^{(n)}(x_{\pm}) = \int_{x_{\pm}}^1 dx_1 f_{\tau}^{(n)}(x_1) G_{\tau \rightarrow h} \left(\frac{x_{\pm}}{x_1} \right). \quad (3)$$

Here τ means the flavour of the valence (or sea) quark or diquark, $f_{\tau}^{(n)}(x_1)$ is the quark distribution function depending on the longitudinal momentum fraction x_1 in the n -Pomeron chain; $G_{\tau \rightarrow h}(z) = z D_{\tau \rightarrow h}(z)$, $D_{\tau \rightarrow h}(z)$ is the FF of a quark (anti-quark) or diquark of flavour τ into a hadron h (charmed or bottom hadron in our case), where $z = x_{\pm}/x_1$. The PDFs and FFs used by the calculations of Eqs.(2,3) are expressed in terms of the Regge trajectories, their intercepts $\alpha_R(0)$ and slopes $\alpha'_R(0)$. All the details of the calculations can be found in [15, 14, 18].

3. Results and discussion

3..1 QGSM results

Some information on the charmonium ($c\bar{c}$) and bottomonium ($b\bar{b}$) Regge trajectories can be found from the data on the charmed and beauty baryon production in pp collisions at high energies. For example, Fig.3 illustrates the sensitivity of the inclusive spectrum $d\sigma/dx$ of the produced charmed baryons Λ_c to different values of the Regge intercept $\alpha_\psi(0)$. Experiment R608 [19], after measuring the decay $\Lambda_c \rightarrow \Lambda^0 + 3\pi$, obtained $(2.84 \pm 0.50 \pm 0.72) \mu\text{b}$ for the cross section of $pp \rightarrow \Lambda^0 + 3\pi + X$ at $|x| > 0.5$ and $\sqrt{s} = 62 \text{ GeV}$. The branching ratio of this decay is $(2.8 \pm 0.7 \pm 1.1)\%$, therefore the cross section of the Λ_c production is $\sigma(|x| > 0.5) = (101 \pm 18 \pm 26) \mu\text{b}$. Theoretical expectation for this cross section is $87.3 \mu\text{b}$ ($\sigma(|x| > 0.5) = 87.3 \mu\text{b}$) with $\alpha_\Psi(0) = 0$ and $30.5 \mu\text{b}$ with $\alpha_\Psi(0) = -2.18$. On the other hand, experiment R422 [20] measured the process $pp \rightarrow e^- \Lambda_c X$ at $|x| > 0.35$. With a large uncertainty the cross section for the process was obtained to be from $(26 \pm 12) \mu\text{b}$ to $(225 \pm 9) \mu\text{b}$ [20]. It seems that the open circles (R608 experiment) in Fig.3 better correspond to our calculations (solid line) at $\alpha_\Psi(0) = 0$.

Unfortunately, there are no available data for the reaction $pp \rightarrow \Lambda_b X$, some predictions for this kind of reactions are presented in [14], where it is shown that all the observables are very sensitive to the value of the intercept $\alpha_\Upsilon(0)$ of the $\Upsilon(b\bar{b})$ Regge trajectory. The upper limit of our results is reached at $\alpha_\Upsilon(0) = 0$, when this Regge trajectory is the nonlinear t -function. In fact, to measure the above-mentioned distributions of the process $pp \rightarrow \Lambda_b X$ one should reliably detect the Λ_b -hyperon. For this purpose, we believe, the beauty baryon decays $\Lambda_b \rightarrow J/\Psi \Lambda^0 \rightarrow \mu^+ \mu^- p \pi^-$ (Fig. 4) and $\Lambda_b \rightarrow J/\Psi \Lambda^0 \rightarrow e^+ e^- n \pi^0$ can be used. The produced Λ_b baryon can undergo the decay $\Lambda_b \rightarrow J/\Psi \Lambda^0$ with the branching ratio $Br_{\Lambda_b \rightarrow J/\Psi \Lambda^0} = \Gamma_{\Lambda_b \rightarrow J/\Psi \Lambda^0} / \Gamma_{tot} = (4.7 \pm 2.8) \cdot 10^{-4}$. The J/Ψ decays into $\mu^+ \mu^-$ ($Br_{J/\Psi \rightarrow \mu^+ \mu^-} = (5.93 \pm 0.06)\%$) or into $e^+ e^-$ ($Br_{J/\Psi \rightarrow e^+ e^-} = (5.94 \pm 0.06)\%$), whereas Λ^0 can decay into $p \pi^-$ ($Br_{\Lambda^0 \rightarrow p \pi^-} = (63.9 \pm 05)\%$), or into $n \pi^0$ ($Br_{\Lambda^0 \rightarrow n \pi^0} = (35.8 \pm 0.5)\%$).

One can experimentally measure the differential cross section of this process $d\sigma/d\xi_p dt_p dM_{J/\Psi}$, where $\xi_p = \Delta p/p$ is the energy loss, $t_p = (p_{in} - p_1)^2$ is the four-momentum transfer, $M_{J/\Psi}$ is the effective mass of the J/Ψ -meson. In principle, the ATLAS and CMS detectors could detect the decay $\Lambda_b^0 \rightarrow J/\Psi \Lambda^0 \rightarrow \mu^+ \mu^- \pi^0 n (\pi^- p)$ by recording two muons and one nucleon (neutron in ATLAS - ZDC and proton in TOTEM) emitted forward. However, the acceptance of the muon detection is $8^0 \leq \theta_\mu \leq 172^0$ [21]-[23], and according to our calculations the fraction of expected events in this region is too low. On the other hand, the electromagnetic calorimetry allows one to measure the dielectron pairs $e^+ e^-$ with acceptance about $1^0 \leq \theta_{e(e^+)} \leq 179^0$ [21]-[23].

In Figs.(5,6) the distributions over the proton scattering angle θ_p in the reactions $pp \rightarrow \Lambda_b X \rightarrow J/\Psi \Lambda_0 X \rightarrow \mu^+ \mu^- p \pi^- X$ and over the neutron scattering angle θ_n in the process $pp \rightarrow \Lambda_b X \rightarrow J/\Psi \Lambda_0 X \rightarrow e^+ e^- \pi^0 n X$ are presented at the intercept

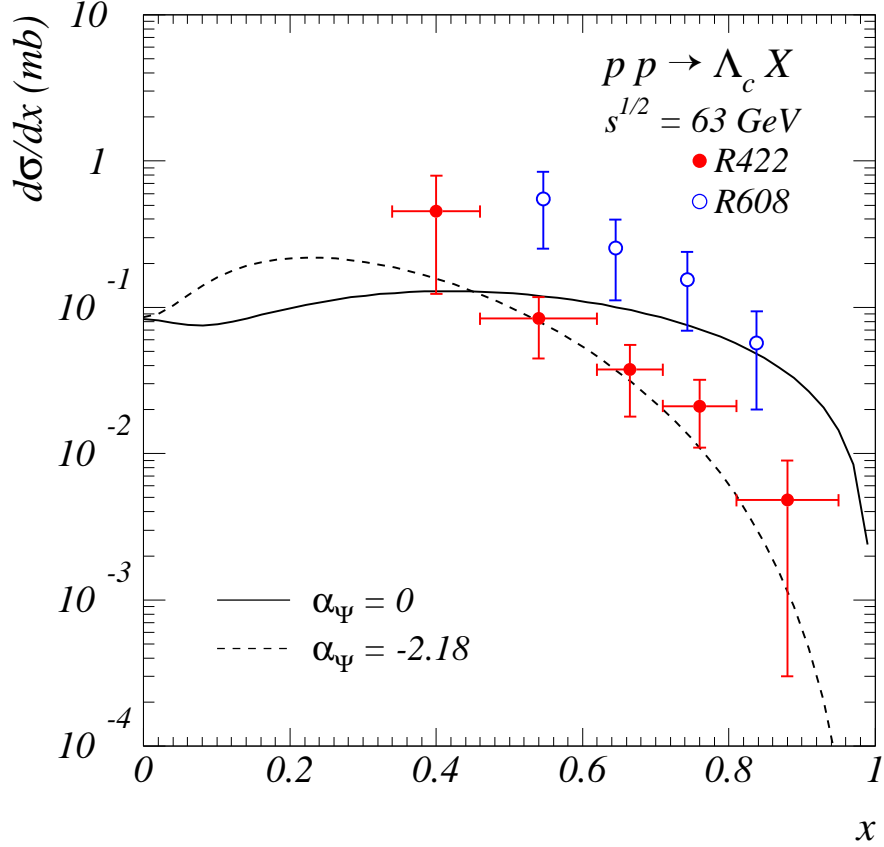


Figure 3: The differential cross section $d\sigma/dx$ for the inclusive process $pp \rightarrow \Lambda_c X$ at $\sqrt{s} = 63$ GeV. The solid line corresponds to $\alpha_\psi(0) = 0$. The dashed curve corresponds to $\alpha_\psi(0) = -2.18$. The open circles correspond to the R608 experiment [19], and the dark circles correspond to the R422 experiment [20].

values $\alpha_\Upsilon(0) = 0$ (solid line) and $\alpha_\Upsilon(0) = -8$ (dashed line). Figures 5,6 show a large sensitivity of these distributions to the intercepts $\alpha_\Upsilon = 0$ and $\alpha_\Upsilon = -8$ of the $\Upsilon(b\bar{b})$ Regge trajectory. One can see that the cross section $d\sigma/d\theta_{p,n}$ for the nonlinear $\Upsilon(b\bar{b})$ Regge trajectory ($\alpha_\Upsilon = 0$) is larger than for the linear one ($\alpha_\Upsilon = -8$). As is shown above for the Λ_c production in pp collisions, the use of the nonlinear $\psi(c\bar{c})$ Regge trajectory results in the better correspondence of the calculations to the experimental data. Therefore, one can assume that all our results obtained at $\alpha_\Upsilon = 0$ are more preferable than the ones at $\alpha_\Upsilon = -8$ and they can be considered as the upper limit of our QGSM calculations. The reaction $pp \rightarrow \Lambda_b X \rightarrow J/\Psi \Lambda_0 X \rightarrow \mu^+ \mu^- (e^+ e^-) p \pi^- X$ can be measured by the TOTEM and CMS, and the neutron produced from the Λ_0 decay can be detected by the ATLAS Zero Degree Calorimeter (ZDC).

In Figs.(7,8) the two-dimensional plots of the energy and scattering angle for the positron (electron) produced in the J/Ψ decay and the neutron produced in the Λ^0

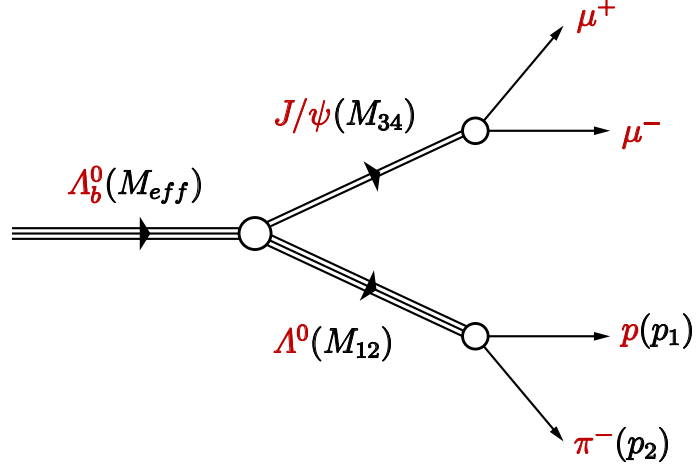


Figure 4: The decay $\Lambda_b \rightarrow J/\Psi \Lambda^0 \rightarrow e^+(\mu^+)e^-(\mu^-)n(p)\pi^0(\pi^-)$.

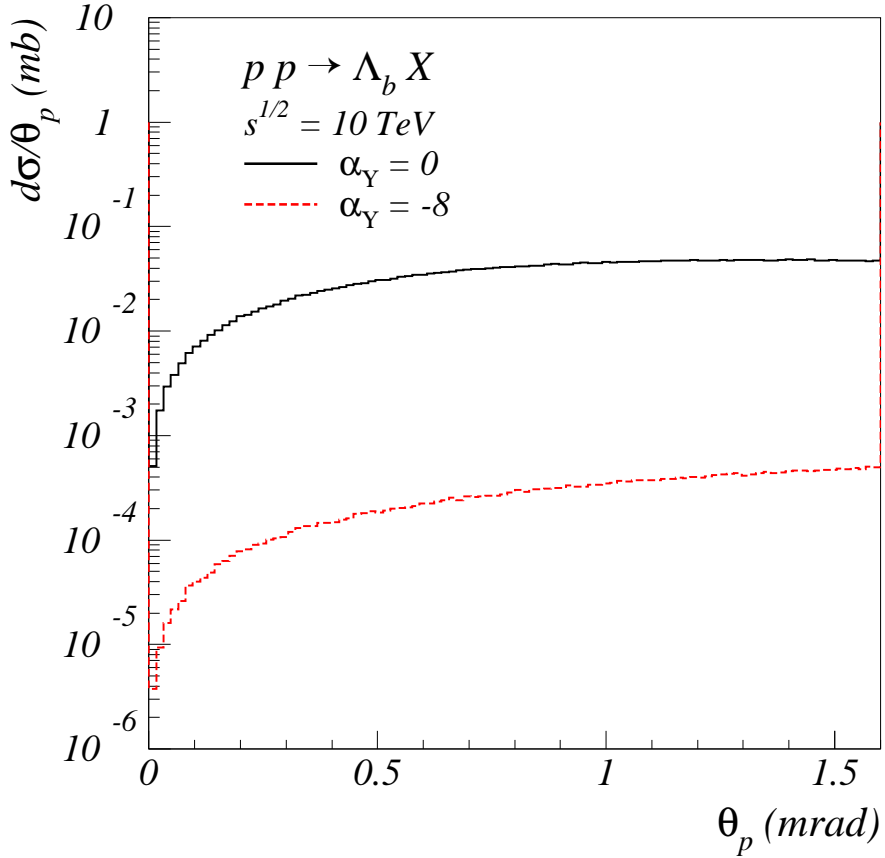


Figure 5: The distributions over θ_p for $pp \rightarrow \Lambda_b X \rightarrow \mu^+ \mu^- p \pi^- X$ at $\sqrt{s} = 10$ TeV. The solid (long dashed) curve corresponds to $\alpha_Y(0) = 0$ ($\alpha_Y(0) = -8$).

decay are presented. These plots correspond to $\alpha_Y = 0$.

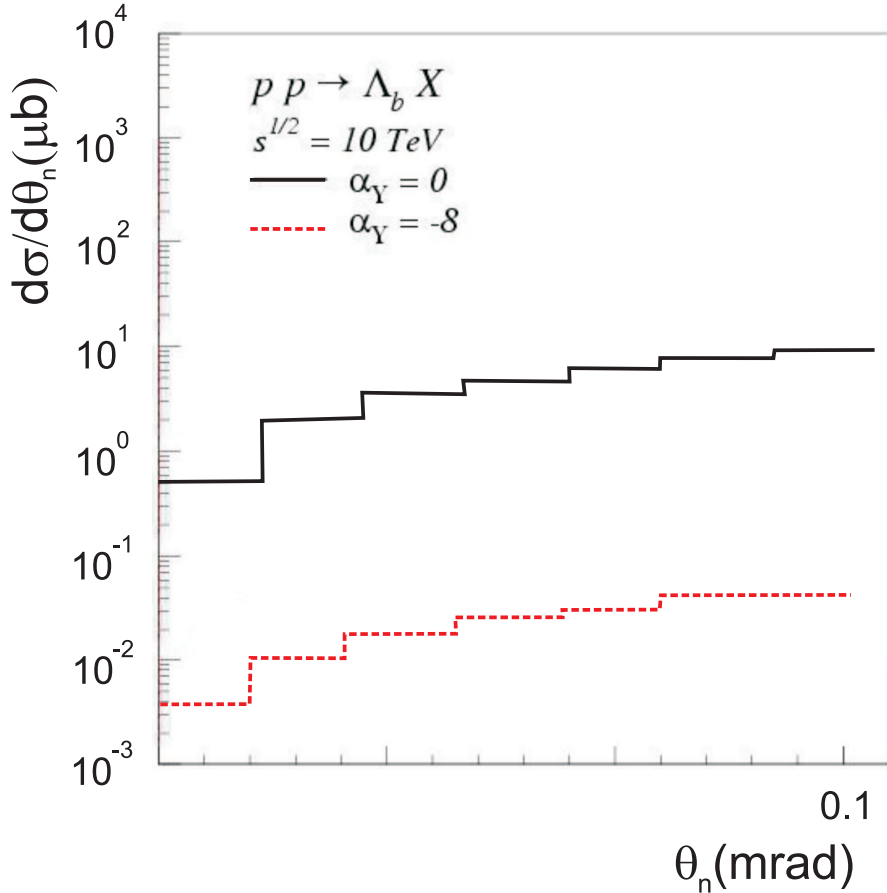


Figure 6: The distribution $d\sigma/d\theta_n$ over the neutron scattering angle θ_n for $pp \rightarrow \Lambda_b X \rightarrow e^+e^-\pi^0n$ at $\sqrt{s} = 10$ TeV. The solid (long dashed) curve corresponds to $\alpha_Y(0) = 0$ ($\alpha_Y(0) = -8$).

One can see from Figs. (7,8) that positrons (electrons) are concentrated at the scattering angles $4 \text{ mrad} < \theta_{e*+} < 16 \text{ mrad}$, whereas the neutrons are emitted mainly at $\theta_n \leq 0.1 \text{ mrad}$ which could be measured with ATLAS using the ZDC (n) or with the TOTEM & CMS (p). The ATLAS experiment is also able to detect e^+e^- by the electromagnetic calorimeter in the interval $1^0 \leq \theta_{e(e^+)} \leq 179^0$ [21]. The ratio of the events presented in Fig. (7) to the total yield (let us call it the rate) is about 4.6 percent (13.8 nb). The detailed analysis and theoretical predictions for the Λ_b production in the forward pp collisions without the inclusion of the possible intrinsic bottom in the proton were presented in [14, 24]. It was shown [24] that the rate of the events in the reaction $pp \rightarrow \Lambda_b \rightarrow J/\Psi \Lambda^0 \rightarrow e^+e^- \pi^-p$ at $\sqrt{s} = 7$ TeV when $500 \text{ GeV} \leq E_p \leq 4 \text{ TeV}$ and the proton scattering angle $3 \text{ mrad} \leq \theta_p \leq 10 \text{ mrad}$ was about 1.33 % (40 nb). In principle, this kinematics corresponds to that of the TOTEM and CMS facilities at CERN. And the rate in the reaction $pp \rightarrow \Lambda_b \rightarrow J/\Psi \Lambda^0 \rightarrow e^+e^- \pi^0n$ at the same initial energy when $E_n \leq 3 \text{ TeV}$

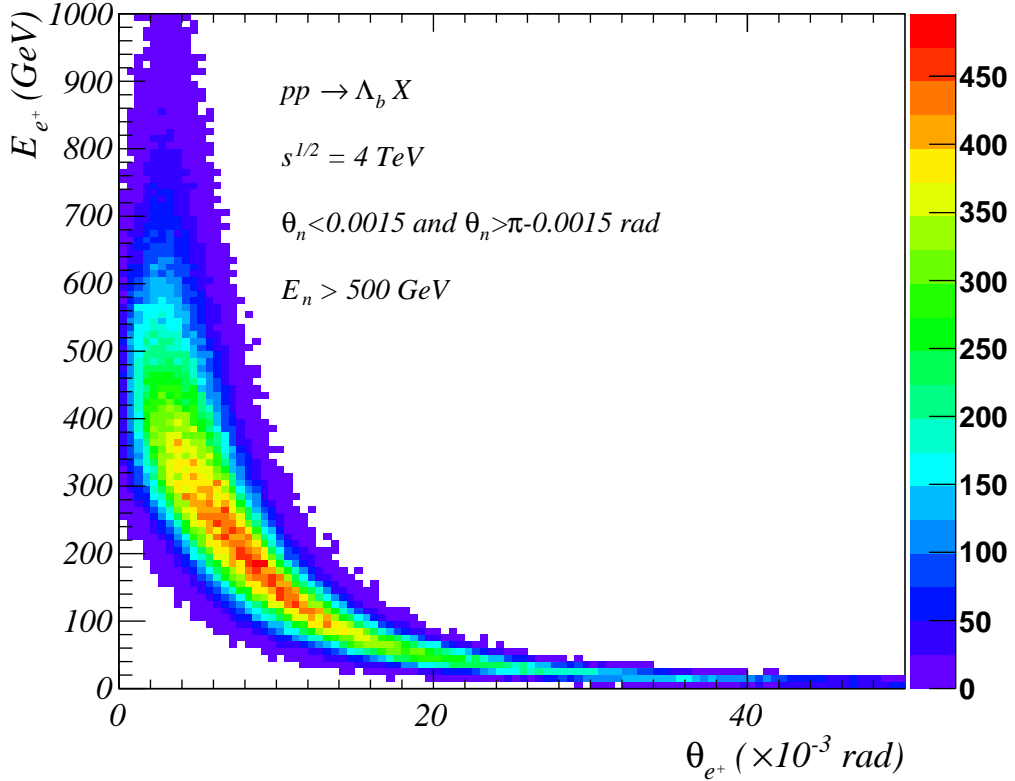


Figure 7: The distributions over θ_{e^+} and E_{e^+} in the inclusive process $pp \rightarrow \Lambda_b X \rightarrow J/\Psi \Lambda^0 X \rightarrow e^+ e^- n \pi^0 X$ at $\sqrt{s} = 4$ TeV. The rate of these events is about 4.6 percent (13.8 nb).

and the neutron scattering angle $\theta_n \leq 0.1$ mrad is about 0.0207 (60. pb). This kinematics corresponds to the ATLAS and ZDC at CERN.

Therefore, we see that the cross section of the Λ_b -hyperon produced in pp collisions and decayed into $\pi^- p$ or $\pi^0 n$ calculated within the QGSM without the intrinsic bottom in the proton can be from 60 pb to 40 nb at the different kinematics of the LHC experiments at $\sqrt{s} = 7$ TeV.

3..2 Intrinsic charm and beauty contribution

Let us discuss the opportunity to find some information on the distributions of intrinsic charm and beauty in the proton from the analysis of the forward production of heavy flavour baryons in pp collisions at the LHC. First, we note that all sea quark distributions in the proton calculated within the QGSM give their contributions only to the multi-Pomeron graphs at $n \geq 2$ (Fig. 2 (right)). According to Eq. (2), they do not contribute to the one-Pomeron graph (Fig. 2 (left)). The one-Pomeron graph results in the main contribution at large values of x because σ_n decreases very fast when n increases [16]. Therefore the sea charm and beauty quark distributions

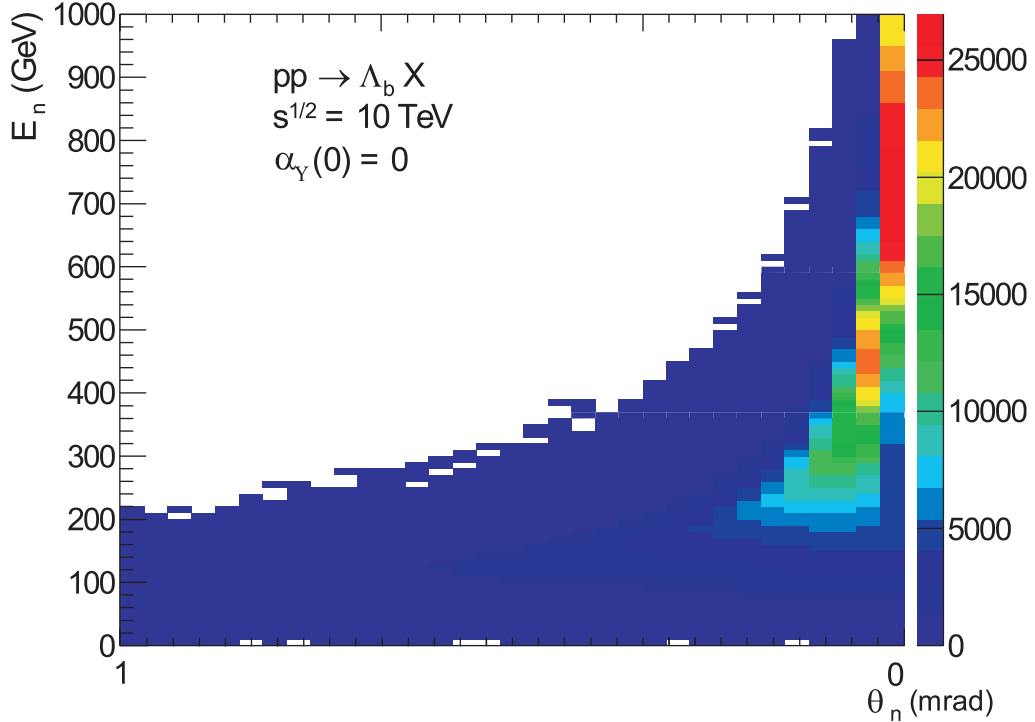


Figure 8: The neutron energy distribution as a function of θ_n for the process $pp \rightarrow \Lambda_b X \rightarrow e^+ e^- \pi^0 n X$ at $\sqrt{s} = 10$ TeV.

result in very small contributions to the inclusive spectra of the charmed and beauty hadrons at not large p_t and different values of x [25, 15, 14]. For the forward heavy flavour hadron production this contribution is smaller and we neglect it.

These *sea* charm and beauty quark distributions greatly differ from the distributions of the *intrinsic* charm and bottom quarks in the proton, which, according to the assumption of [10, 3], should behave like the *valence* quark distributions. Therefore, if one wants to estimate the contribution of the intrinsic charm and bottom quarks within the QGSM scheme, one should include their distributions in the calculation of the one-Pomeron graph ($n = 1$). The procedure can increase the rates of events for both reactions $pp \rightarrow \Lambda_b X \rightarrow e^+ e^- p \pi^- X$ and $pp \rightarrow \Lambda_b X \rightarrow e^+ e^- n \pi^0 X$ when the final proton or neutron is emitted in the forward direction because the one-Pomeron graph (Fig. 2 (left)) makes the major contribution to the Λ_b spectrum in this kinematics.

Assuming the existence of the intrinsic $b\bar{b}$ -pair in the proton, as a pair of the *valence* quark-antiquark, with some non-zero probability $w_{b\bar{b}}$, one can estimate enhancement in the forward Λ_b pp -production at the LHC. The expected enhancement will be about the ratio of the differential cross sections $\frac{d\sigma}{dx}(pp \rightarrow n X) / \frac{d\sigma}{dx}(pp \rightarrow \Lambda_b X)$ at very large x multiplied by $w_{b\bar{b}}$. Although it is suppressed in comparison with the intrinsic charm probability $w_{c\bar{c}}$ by a factor $m_c^2/m_b^2 \simeq 0.1$ [12], it can not be neglected

nevertheless.

Calculating these spectra within the QGSM [17, 14, 15] at large x and assuming $w_{b\bar{b}} \sim 0.3\%$ [5, 12] one can get that the yield of Λ_b produced hadronically in the forward direction can increase by a factor 3-5 times due to the intrinsic bottom quark contribution. It means that the cross section of the forward production of Λ_b in pp collisions at LHC energies, which decays into $e^+e^-\pi^-p$ or $e^+e^-\pi^0n$, can reach a few hundred nb for TOTEM and CMS and few hundred pb for ATLAS. Our estimations show that the yield of the forward charmed Λ_c^+ -hyperon production can be increased by a factor of 10 due to the intrinsic charm quarks. Therefore, the reaction $pp \rightarrow \Lambda_c^+ X \rightarrow \Lambda^0 \pi^+ X \rightarrow n \pi^0 \pi^+ X$ can also be measured at the LHC when the neutron is emitted in the forward direction. The neutron can be measured by the ZDC and π^+ -meson can be detected by the hadron calorimeter. We presented

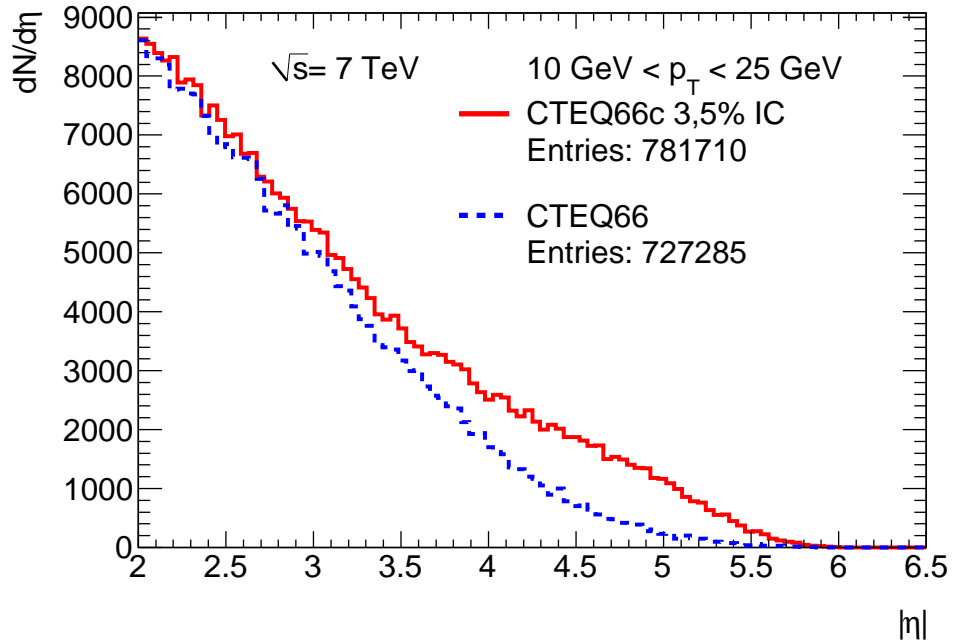


Figure 9: The $D + \bar{D}_0$ distributions over the pseudo-rapidity η in $pp \rightarrow (D_0 + \bar{D}_0)X$ at $\sqrt{s} = 7$ TeV and $10 \leq p_t \leq 25$ GeV/c.

the qualitative estimations for the contributions of the intrinsic beauty and charm to the forward Λ_b and Λ_c production at LHC. These spectra were calculated within the nonperturbative QGSM in which the PDF do not include the intrinsic charm or beauty contributions. It is not so easy to take into account the intrinsic charm (IC) contribution at the PDF used in the QGSM [1, 17].

However, there are the PDF used in the perturbative QCD calculations which include the IC contribution in the proton [3]-[5]. The probability distribution for the 5-quark state ($uudcc\bar{c}$) in the light-cone description of the proton was first calculated

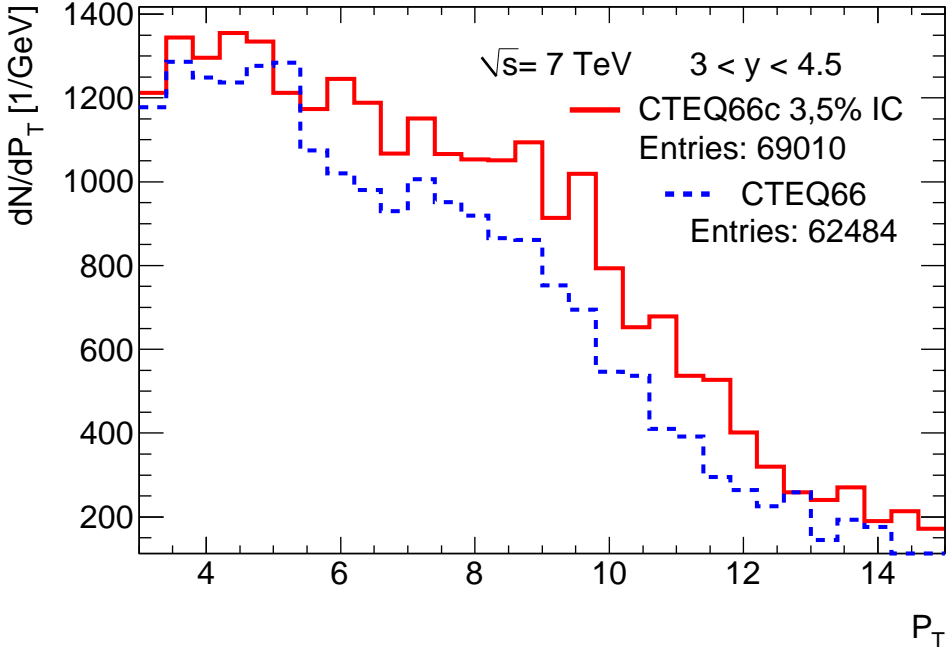


Figure 10: The double D^0 distributions over the pseudo-rapidity η in $pp \rightarrow (D_0 + \bar{D}_0)X$ and at $p_t \geq 25$ GeV/c.

in [10]. It has the following form [4]

$$\frac{dP}{dx} = f_c(x) = f_{\bar{c}}(x) = \mathcal{N} 6x^2 \times \left\{ (1-x)(1+10x+x^2+6x\ln(x)) \right\}, \quad (4)$$

where \mathcal{N} is the normalization constant. One can see from Eq.(4) that the IC distribution has some enhancement at large x and vanishes at $x = 1$. As is shown in [5] this enhancement starts at $x > 0.2$ that can result in similar enhancement in the inclusive spectra of the open charm at large rapidities y or pseudorapidities η and transverse momenta p_t . We calculated the IC contribution to the inclusive spectra of the D -mesons produced in pp collisions at $\sqrt{s} = 7$ TeV within the perturbative QCD. In Fig.9 the inclusive spectrum of single D^0 -mesons is presented as a function of the pseudorapidity η at $10 \text{ GeV}/c < p_t < 25 \text{ GeV}/c$. Calculating these spectra within PYTHIA8 we used the PDF both for the CTEQ66 without the IC (the dashed blue distributions in Fig.9) and the CTEQ66c including the IC with the probability about 3.5 % (the solid red distributions in Fig.(9)) at $Q^2 = m_c^2 = 1.69 \text{ GeV}^2$ [5]. Figure 9 shows that some enhancement due to the IC can be visible at large η . Its amount increases when p_t grows and, for example, the inclusion of the IC increases the spectrum by a factor of 2 at $\eta = 4.5$. Similar effect was predicted in [26]. In Fig.10 the inclusive spectrum of the D^0 -meson produced in the process

$pp \rightarrow D^0 D^0 X$ at the rapidity interval $3 < y < 4.5$ and $\sqrt{s} = 7$ TeV is presented as a function of p_t , when two D^0 are produced. The enhancement of the spectrum (the excess of the solid histogram in comparison to the dashed one) at $7 < p_t < 10$ GeV/c is not more than 30 %. The predictions presented in Figs.(9,10) can be verified by the LHCb experiment at CERN because their facility is able to measure inclusive spectra of D -mesons at $\eta \leq 4.5$.

4. Conclusion

We analyzed production of charmed and beauty baryons in proton-proton collisions at high energies within the soft QCD quark-gluon string model. This approach described rather satisfactorily the charmed baryon production in pp collisions [15, 14] and allowed us to apply the QGSM to beauty baryon production. We focus mainly on the analysis of the forward Λ_b production in pp collisions at LHC energies. We present the predictions for the reaction $pp \rightarrow \Lambda_b X \rightarrow e^+ e^- n\pi^0 X$, which can be studied in the ATLAS experiment using the ZDC, and for the process $pp \rightarrow \Lambda_b X \rightarrow e^+ e^- p\pi^- X$, which could be reliably studied at the TOTEM and CMS within their common proposal for Diffractive and Forward Physics at the LHC [22, 23]. We show that beauty Λ_b -hyperons can in principle be detected in LHC experiments via registration of their decay products $\Lambda_b \rightarrow e^+ e^- p\pi^-$ and $\Lambda_b \rightarrow e^+ e^- n\pi^0$.

We would like to stress that any data on forward production in the process $pp \rightarrow \Lambda_b X$ could be important for determination of $\alpha_\Upsilon(0)$ of the $\Upsilon(b\bar{b})$ Regge trajectory. Our predictions with the nonlinear Regge trajectories of $c\bar{c}$ and $b\bar{b}$ mesons can be considered as the upper limit of the QGSM calculations without the intrinsic charm and bottom in the proton.

The inclusion of the intrinsic bottom or/and charm in the proton can increase the yield of the relevant heavy flavour baryons by a factor of 3 to 10. In particular, we considered a possibility of measuring the reaction $pp \rightarrow \Lambda_c^+ X \rightarrow \Lambda^0 \pi^+ X \rightarrow n\pi^0 \pi^+ X$ using the ATLAS (ZDC). This measurement can provide information on the intrinsic charm in the proton, the probability of which is estimated to be a factor of 10 higher than the one for the intrinsic bottom in the proton. Finally, it is worth noticing that any reliable non-observation of this enhancement in the experiments at the LHC can severely constrain the intrinsic heavy quark hypothesis.

Our calculations of the charmed meson production in pp collisions within the MC generator PYTHIA8 and the PDF including the intrinsic charm showed the following. We found that the contribution of the intrinsic charm in the proton could be studied in the production of D -mesons in pp collisions at the LHC. The IC contribution for the single D^0 -meson production can be sizable, it is about 100 % at large rapidities $3 \leq y \leq 4.5$ and large transverse momenta $10 \leq p_t \leq 25$ GeV/c. For the double D^0 production this contribution is not larger than 30 % at $p_t \geq 5$ GeV/c and $3 \leq y \leq 4.5$. These IC contributions for the single and double D -meson production were obtained with the probability of the intrinsic charm taking to be

$w_{c\bar{c}} = 3.5\%$ [5], and they will decrease by a factor of 3 when $w_{c\bar{c}} \simeq 1\%$. Therefore, this value can be verified experimentally at LHCb.

The presented predictions could stimulate measurement of the single and double D-meson production in pp collisions at the CERN LHCb experiment in the kinematic region mentioned above to observe a possible signal for the intrinsic charm. The intrinsic beauty in the proton is suppressed by a factor of 10, therefore its signal in the inclusive spectra of B -mesons will probably be very weak.

5. Acknowledgments

We are very grateful to V.V. Lyubushkin and D.A. Artemenkov for their help with the MC calculations. We also thank M. Deile for extremely useful suggestions related to the possible experimental check of our predictions at the LHC. We are also grateful to I.Belyaev, V.Gligorov, D.Denegri, K. Eggert, H.Jung, B.Kniehl, S.Lami, T.Lomtadze, A.Likhoded, F.Palla, P.Spradlin, O.V.Teryaev, M. Poghosyan and S.White for very useful discussions. This work was supported in part by the Russian Foundation for Basic Research grant N: 11-02-01538-a.

References

- [1] Kaidalov A. B., Phys.Lett. B **116** (1982) 459.
- [2] Capella A., Sukhatme U., Tan C.-I., Tran Thanh Van J., Phys.Rept. **236** (1994) 225.
- [3] Pumplin J., Phys.Rev. D **73** (2006) 114015.
- [4] Pumplin J., Lai H., Tung W., Phys.Rev. D **75** (2007) 054029.
- [5] Nadolsky P. M., *et. al.*, Phys. Rev. D **78** (2008) 013004.
- [6] Litvine V. A., Likhoded A. K., Phys. Atom. Nucl. **62** (1999) 679.
- [7] Vogt R., Prog. Part. Nucl. Phys. **45** (2000) S105.
- [8] Navarra F. S., Nielsen M., Nunes C. A. A., Teixeira M., Phys.Rev. D **54** (1996) 842.
- [9] Melnichouk W., Thomas A. W., Phys.Lett. B **414** (1997) 134.
- [10] Brodsky S., Hoyer P., Peterson C., Sakai N., Phys.Lett. B **93** (1980) 451.
- [11] Brodsky S., Peterson C., Sakai N., Phys.Rev. D, **23** (1981) 2745.
- [12] Polyakov M. V., Schafer A., Teryaev O. V., Phys.Rev. D **60** (1999) 051502.

- [13] Goncalves V., Navarra F., Nucl.Phys. A **842** (2010) 59.
- [14] Bednyakov V. A., Lykasov G. I., Lyubushkin V. V., Europhys.Lett. **92** (2010) 31001.
- [15] Lykasov G. I., Lyubushkin V. V., Bednyakov V. A., Nucl.Phys.[Proc.Suppl.] **198** (2010) 165.
- [16] Ter-Martirosyan K. A., Phys.Lett. B **44** (1973) 377.
- [17] Kaidalov A. B., Piskunova O. I., Z.Phys. C **30** (1986) 145.
- [18] Bednyakov V., Grinyuk A., Lykasov G., Poghosyan M., Int.J.Mod.Phys. A**27** (2012) 1250042.
- [19] Chauvat P. *et.al.*, Phys.Lett. B **199** (1987) 304.
- [20] Bari G., Basile M., Bruni G., Cara Romeo G., Casaccia R., *et.al.*, Nuovo Cim. A **104** (1991) 571.
- [21] ATLAS Collaboration, *Thechnical Design Report* ATLAS-TDR-017 CERN-LHCC (2005) 022.
- [22] CMS Collaboration, Khachatryan V. *et.al.*, JHEP **02** (2010) 041.
- [23] TOTEM Collaboration *Thechnical Design Report* CERN-LHCC-002 (2004) .
- [24] Lykasov G. I., Artyukhov D. A., Bednyakov V. A., *Proc. of XI Int.Symp.Multiparticle Dynamics* **1** (2010) 269.
- [25] Lykasov G. I., Karpova Z. M., Sergeenko M. N., Bednyakov V. A., Europhys.Lett. **86** (2009) 61001.
- [26] Kniehl B., Kramer G., Schienbein I. and Spiesberger H., ArXiv:1202.0439v1 (2012) [hep-ph] .